Systematics and Biodiversity (2019), **17(4)**: 349–366

Taylor & Francis
Taylor & Francis Group

Research Article

Systematics, biogeography, and evolution of *Pristurus minimus* (Squamata, Sphaerodactylidae) with the discovery of the smallest Arabian vertebrate

KARIN TAMAR[1]*, PELAGIA MITSI[1]*, MARC SIMÓ-RIUDALBAS[1], HéCTOR TEJERO-CICUéNDEZ[1], THURAYA AL-SARIRI[2] & SALVADOR CARRANZA[1]

[1]Institute of Evolutionary Biology (CSIC-Universitat Pompeu Fabra), Passeig Maritim de la Barceloneta, 37–49, Barcelona, 08003, Spain
[2]Ministry of Environment and Climate Affairs, Thaqafah Street, 100, Muscat, Oman

(Received 22 January 2019; accepted 23 April 2019)

Almost 20% of Oman's terrestrial reptiles are found on Masirah Island. Despite its ancient geological history and its long isolation, Masirah Island only harbours one endemic reptile species, *Hemidactylus masirahensis*. In this study, we use an integrative approach to explore the variation in *Pristurus minimus*, to revise its systematics and to assess its phylogeography by using molecular (mitochondrial and nuclear DNA sequences) and morphological data. Our results uncovered a deep divergence within *P. minimus* that dates back to ~4 Ma, during the Pliocene Epoch. The old divergence separated *P. minimus* into two allopatric species: one from mainland Arabia, *P. minimus*, and one endemic to Masirah Island, described as a new species herein. Despite the general similarity between the two sister species, there are morphological differences related mainly to body size. The new *Pristurus* species endemic to Masirah Island is significantly smaller than its mainland sister taxon, becoming the smallest known vertebrate species in Arabia and one of the smallest lizard species in the world. The phylogenetic analyses also uncovered a low level of genetic diversity within the newly described *Pristurus* species endemic to Masirah Island and a relatively deep genetic divergence within *P. minimus* that dates back to the Pleistocene. Once more, the present study highlights the relatively high levels of reptile diversity and endemicity in south-eastern Arabia despite its harsh, arid climate and stresses its relevance from a conservation point of view.

The LSIDs for this publication is: urn:lsid:zoobank.org:pub:DB0658D5-7F68-4E66-885F-75E27F9CD512.

Keywords: allopatric speciation, body size, geographic isolation, islands, phylogeography, species delimitation

Introduction

With an area of about 700 km^2, 65 km in length and up to 15 km at its widest, Masirah Island is the largest island of Oman (Carranza et al., 2018; Edgell, 2006). It is located in the Arabian Sea, near the south-east corner of the Arabian Peninsula (Fig. 1). The island is 14.3 km off the north-east coast of Oman, separated from the mainland by the shallow and narrow Masirah Fault, which separates the continental Arabian plate (mainland) from the Indian oceanic crust, represented by the Masirah Island ophiolite and the other ophiolites along the eastern coast of Oman (Shackleton & Ries, 1990 and see references therein). The Masirah Ophiolite is structurally part of the Indian Ocean floor (i.e., ophiolite block uplifted and moved by obduction onto the Arabian Shelf) and geochemically different from the Semail Ophiolite from northern Oman, thus the island is not geologically related to the continent (Moseley, 1969, 1990; Moseley & Abbotts, 1979; Rollinson, 2017). Masirah Island is suggested to have originated during the Early Cretaceous with the over-thrust at the mid-end of the Cretaceous, emplaced on the margin of north-eastern Oman (Edgell, 2006; Immenhauser, 1996; Shackleton & Ries, 1990; Smewing, Abbotts, Dunne, & Rex, 1991).

Correspondence to: Salvador Carranza. E-mail: salvador.carranza@ibe.upf-csic.es
*These authors contributed equally to this work.

ISSN 1477-2000 print / 1478-0933 online
© The Trustees of the Natural History Museum, London 2019. All Rights Reserved.
https://dx.doi.org/10.1080/14772000.2019.1614694

Masirah Island has a significant diversity of reptiles. Nineteen of the 101 species of Oman's terrestrial reptiles are found on the island (Carranza et al., 2018). Most of these species occur on the island in addition to their mainland range, such as *Acanthodactylus masirae* Arnold (Tamar et al., 2016a), *Stenodactylus leptocosymbotes* Leviton & Anderson (Metallinou et al., 2012), *Trachydactylus hajarensis* (Arnold) (de Pous et al., 2016), and *Uromastyx thomasi* Parker (Tamar et al., 2018). Surprisingly, despite its long period of isolation, Masirah Island only harbours a single endemic species, *Hemidactylus masirahensis* (Carranza et al., 2018; Carranza & Arnold, 2012).

The genus *Pristurus* Rüppell currently consists of 25 described species, distributed mainly across Arabia, the Socotra Archipelago and north-east Africa, with one isolated species in Mauritania and another which extends from Arabia to the west coast of Iran (Arnold, 2009; Sindaco & Jeremčenko, 2008; Uetz, Freed, & Hošek, 2019). *Pristurus* has been relatively understudied, especially when compared with other gecko genera from the same region, such as *Hemidactylus*, *Stenodactylus*, and *Asaccus* (e.g., Carranza, Simó-Riudalbas, Jayasinghe, Wilms, & Els, 2016; Carranza & Arnold, 2012; Fujita & Papenfuss, 2011; Gómez-Díaz, Sindaco, Pupin, Fasola, & Carranza, 2012; Metallinou et al., 2012; Metallinou & Carranza, 2013; Metallinou & Crochet, 2013; Šmíd, Shobrak, Wilms, Joger, & Carranza, 2017; Šmíd et al., 2013a, 2013b, 2015; Simó-Riudalbas, Tarroso, Papenfuss, Al-Sariri, & Carranza, 2018; Tamar, Mitsi, & Carranza, 2019; Vasconcelos & Carranza, 2014). The morphology-based phylogeny of 20 species of *Pristurus* by Arnold (2009) recovered a clade of nine species (i.e., *P. carteri* (Gray); *P. collaris* (Steindachner); *P. crucifer* (Valenciennes); *P. minimus* Arnold; *P. ornithocephalus* Arnold; *P. phillipsi* Boulenger; *P. saada* Arnold; *P. simonettai* (Lanza and Sassi); and *P. somalicus* Parker) distributed across the gravelly and sandy plains of the Horn of Africa and south-east Arabia, which was assigned the name *Spatalura* Gray. The members of the *Spatalura* clade differ from the other *Pristurus* species in several morphological characters, but also in their ecology and behaviour, being ground dwelling and partly nocturnal as opposed to rock or tree climbers, and inhabiting flat open areas with sparse vegetation that is used as refuge by some of the species (Arnold, 2009). Remarkably, the monophyly of the *Spatalura* clade has been supported in all the molecular phylogenetic studies targeting the genus *Pristurus* carried out to date (Badiane et al., 2014; Garcia-Porta, Simó-Riudalbas, Robinson, & Carranza, 2017; Papenfuss et al., 2009). Within the *Spatalura* clade, the species *Pristurus minimus* is the sister taxon to all the remaining species (Badiane et al., 2014; Garcia-Porta et al., 2017; Papenfuss et al., 2009).

Pristurus minimus is the smallest species in the genus – it measures less than 30 mm from snout to vent (Arnold, 1977, 2009). This species is distributed mainly across most of Oman, including Masirah Island, with one record from southern Saudi Arabia, one from extreme eastern Yemen (near the Oman border), and several populations in north-eastern United Arab Emirates (UAE) (Arnold, 1977, 1980; Burriel-Carranza et al., 2019; Carranza et al., 2018; Gallagher & Arnold, 1988; Gardner, 2013; Sindaco & Jeremčenko, 2008). *Pristurus minimus* is typically found on flattish, sandy substrate or on sand hummocks, and it can be seen in open areas, around low shrubs, which can be dense and woody (Gardner, 2013). Although it is mostly diurnal, it is also active during the night, taking refuge in vegetation (Arnold, 1977, 1993; Gallagher & Arnold, 1988; Gardner, 2013). The first specimens of *P. minimus* from Masirah Island were collected in 1971 by M.C. Jennings and reported by Arnold (1977), who noticed that they were smaller and more slender than the mainland specimens. Despite these morphological differences, Arnold (1977) included six specimens of *P. minimus* from Masirah Island as paratypes in its original description. Interestingly, in the only molecular phylogenetic study so far that included more than one specimen of *P. minimus*, the species was recovered as monophyletic with high bootstrap support, but with a deep divergence between three specimens from mainland Arabia and two specimens from Masirah Island (Badiane et al., 2014). Despite the apparent morphological and genetic differences, no study has yet assessed the intraspecific variation within *P. minimus* including an appropriate sampling covering most of its known distribution range.

In this study, we used an integrative approach combining molecular and morphological data in order to assess the systematics and biogeography of *P. minimus* and to fully understand the intraspecific differentiation between the populations from mainland Arabia and Masirah Island. We conducted phylogenetic and species delimitation analyses including specimens from across most of the distribution range of *P. minimus* in mainland Arabia and from Masirah Island, and examined its morphological variability. Our molecular and morphological analyses revealed two well-differentiated evolutionary lineages: one including the populations from mainland Arabia and the other endemic to Masirah Island; the latter lineage is described as a new species herein.

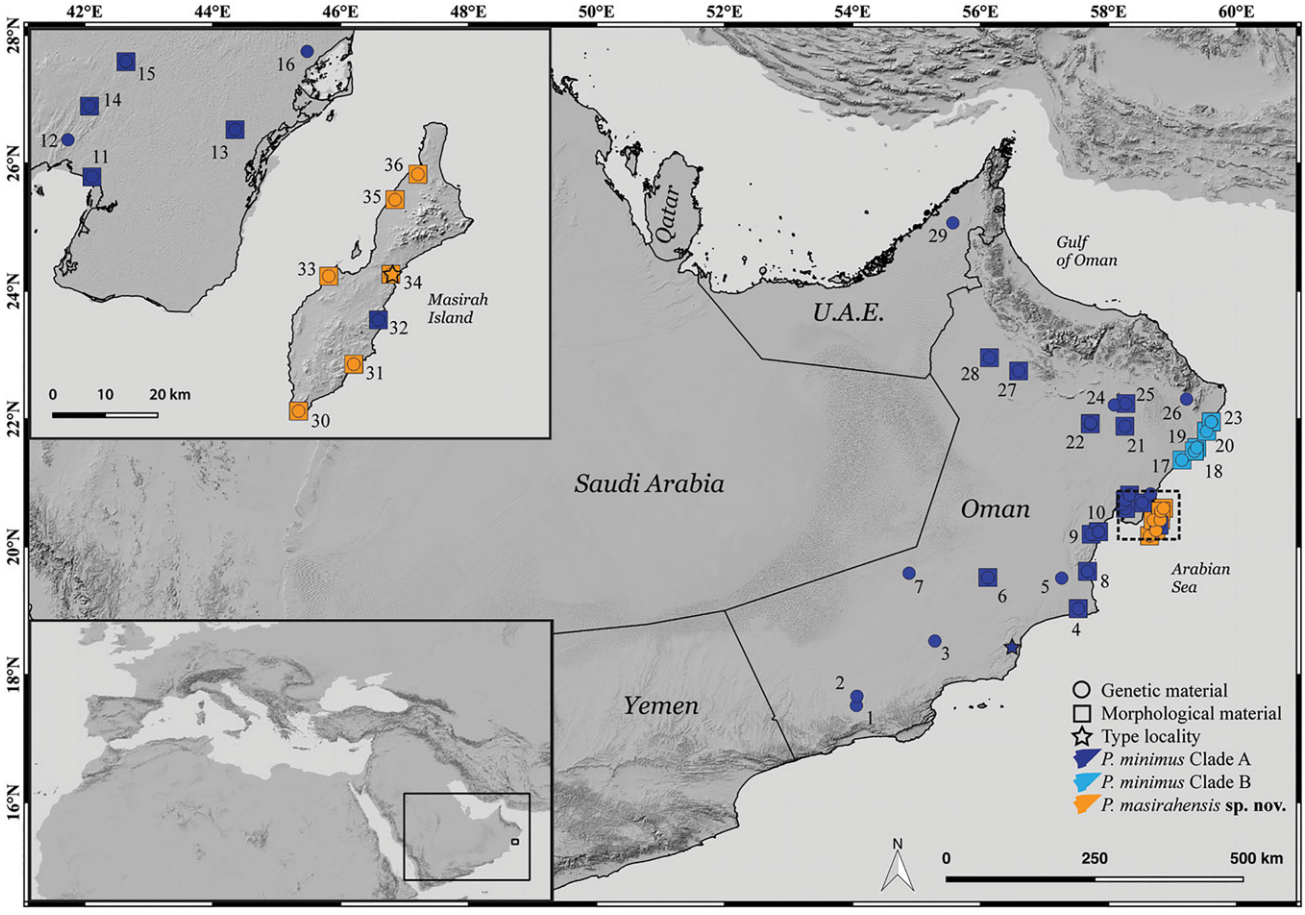

Fig. 1. Localities of the material examined in this study. For *Pristurus masirahensis* sp. nov. (orange symbols) and *Pristurus minimus* (blue symbols), the type localities (stars), samples used for the genetic analyses (circles), and voucher specimens (squares) are shown. Taxon names correspond to changes proposed in this paper. Localities correlate to specimens in Table S1 and colours correspond to those in Figs 2, 3.

Materials and methods

DNA extraction, amplification, and sequence analysis

We included a total of 71 individuals of *Pristurus minimus* from 36 different localities in the molecular study (sequences of five specimens were retrieved from GenBank, from Badiane et al., 2014): 53 specimens were from the mainland (Oman and the UAE) and 18 from Masirah Island. We retrieved from GenBank additional sequences of the available *Spatalura* members to root the phylogenetic trees (using only *P. carteri*) and for the divergence time estimations (using *P. carteri*, *P. collaris*, *P. crucifer*, and *P. somalicus*). Sample information is presented in Table S1 (see supplemental material online, which is available from the article's Taylor & Francis Online page at http://dx.doi.org/10.1080/14772000.2019.1614694) and localities are shown in Fig. 1.

Total genomic DNA was extracted from ethanol-preserved tissue samples using the SpeedTools Tissue DNA Extraction kit (Biotools, Madrid, Spain). We PCR-amplified and sequenced four loci: one mitochondrial gene fragment of the ribosomal 12S rRNA (*12S*) and three nuclear loci, the acetylcholine receptor M4 (*ACM4*), the oocyte maturation factor Mos (*c-mos*), and the melano-cortin 1 receptor (*MC1R*). Primers and PCR conditions for the amplification and sequencing of all the markers were the same as listed in Tamar et al. (2019). Chromatographs were checked, assembled and edited using Geneious v.7.1.9 (Biomatter Ltd). For the nuclear genes, heterozygous positions were identified and coded according to the IUPAC ambiguity codes. We tested the occurrence of recombination for each phased nuclear gene alignment (see below) using the Pairwise Homoplasy Index (PhiTest; Bruen, Hervé, & Bryant, 2006) implemented in SplitsTree v.4.14.5 (Huson & Bryant, 2006) and no evidence of recombination was detected ($P > 0.6$ for each gene). We translated protein-coding genes to amino acids and no stop codons were detected. We aligned the sequences for

each marker using MAFFT v.7.3 (Katoh & Standley, 2013) with default parameters. For the *12S* fragments we applied the Q-INS-i strategy in which data on the secondary structure of the RNA are considered.

Phylogenetic and network analyses

We selected the partitions and substitution models for the phylogenetic analyses using PartitionFinder v.2 (Lanfear, Frandsen, Wright, Senfeld, & Calcott, 2016) with the following parameters: linked branch length; BEAST models; BIC model selection; greedy schemes search algorithm; single partition for the *12S*, and by codons for the protein coding genes *ACM4*, *c-mos*, and *MC1R*. Phylogenetic analyses were performed under Maximum likelihood (ML) and Bayesian (BI) frameworks. We treated alignment gaps as missing data, and the nuclear gene sequences were not phased. We analysed the data with the following partitions and relevant models: *12S* (HKY + G), *MC1R*_1+*ACM4*_1+*ACM4*_2 (TrN + I + G), *c-mos*_1+*c-mos*_2+*c-mos*_3+*ACM4*_3 (K80), *MC1R*_2 (HKY), and *MC1R*_3 (HKY + I + G). We performed the ML analyses in RAxML v.8.1.2 as implemented in raxmlGUI v.1.5 (Silvestro & Michalak, 2012), with the GTRGAMMA model and 100 random addition replicates. Nodal support was assessed with 1,000 bootstrap replicates. We carried out the BI analyses with MrBayes v.3.2.6 (Ronquist et al., 2012). Nucleotide substitution model parameters were unlinked across partitions and the different partitions were allowed to evolve at different rates. Two simultaneous parallel runs were performed with four chains per run (three heated, one cold) for 5×10^6 generations with sampling frequency of every 500 generations. We examined the standard deviation of the split frequencies between the two runs and the Potential Scale Reduction Factor (PSRF) diagnostic; convergence was assessed by confirming that all parameters had reached stationarity and had sufficient effective sample sizes (>200) using Tracer v.1.6 (Rambaut, Suchard, Xie, & Drummond, 2014). We conservatively discarded the first 25% of trees as burn-in. Nodes were considered as well-supported if they received ML bootstrap values ≥70% and posterior probability (pp) support values ≥0.95.

We inferred genealogical relationships among the haplotypes of the lineages detected within *P. minimus* (according to bGMYC and BP&P results, see below) using the phased nuclear sequences. To resolve multiple heterozygous single nucleotide polymorphisms in the nuclear genes, we first used the online web tool SeqPHASE (Flot, 2010) to convert the input files and then the software PHASE v.2.1.1 (Stephens, Smith, & Donnelly, 2001; Stephens & Scheet, 2005) to obtain phased haplotypes with a probability threshold of 0.9 for *c-mos* and 0.5 for *ACM4* and *MC1R*. We then used the TCS statistical parsimony network approach (Clement, Posada, & Crandall, 2000) implemented in the software PopART (Leigh & Bryant, 2015) to generate the networks.

We calculated inter- and intraspecific uncorrected *p*-distance between and within clades of *P. minimus* for the *12S* mitochondrial fragment, with pairwise deletion, in MEGA v.7 (Kumar, Stecher, & Tamura, 2016).

Species delimitation, species tree, and estimation of divergence times

We delimited distinct lineages within *Pristurus minimus* using two sources of information, mitochondrial and nuclear data. To detect divergent mitochondrial lineages we used the ML and BI functions of the Generalized Mixed Yule-Coalescent analysis (GMYC and bGMYC, respectively; Fujisawa & Barraclough, 2013; Pons et al., 2006; Reid & Carstens, 2012) in R v.3.5 (R Development Core Team, 2018). For these analyses we reconstructed a *12S* haplotype tree using BEAST v.1.8.4 (Drummond, Suchard, Xie, & Rambaut, 2012). We set the analysis with the following priors (otherwise by default): HKY + G model, Yule process tree model, random starting tree, uncorrelated relaxed clock (uniform distribution; mean 1, 0–1). Three individual runs of 10^7 generations were carried out, with sampling at intervals of every 10^4 generations. Convergence, posterior trace plots, effective sample sizes (>200), and burn-in were evaluated with Tracer. The three runs were combined in LogCombiner discarding the first 10% as burn-in and the ultrametric tree was generated with TreeAnnotator. For the GMYC analysis we used the 'splits' package (Ezard, Fujisawa, & Barraclough, 2009) applying a single threshold algorithm. Because inference of lineages relies on point estimates of the topology and branch lengths, the associated phylogenetic error could decrease the accuracy of the delimitation results. Therefore, uncertainty in the phylogenetic tree estimation and model parameters were also assessed with bGMYC, which integrates these potential sources of error via MCMC simulation (Reid & Carstens, 2012). For bGMYC we used the 'bGMYC' package (Reid & Carstens, 2012) to calculate marginal posterior probabilities of lineage limits from the posterior distribution of the *12S* ultrametric trees reconstructed with BEAST. A post-burn-in sample of 250 trees resampled from that posterior was used to calculate the posterior distribution of the GMYC model, running the bGMYC analysis for 10^7 generations with a 10% burn-in.

To validate the mitochondrial lineages found within *P. minimus* we performed multilocus Bayesian coalescent species delimitation and species tree analyses using Bayesian Phylogenetics and Phylogeography v.3.3 (BP&P; Rannala & Yang, 2003; Yang & Rannala, 2010) with the phased nuclear loci only. We carried out two analytical approaches setting the initial number of lineages to three (recovered from the bGMYC analysis, see Results): (i) conducting Bayesian species delimitation analysis using a fixed guide tree (with the topology obtained using the concatenated dataset), (ii) implementing a joint analysis conducting Bayesian species delimitation while estimating the species tree (Yang, 2015). For each analysis, we used algorithms 0 and 1, assigning each species delimitation model equal prior probability. As prior distributions on the ancestral population size (θ) and root age (τ) can affect the posterior probabilities for models (Yang & Rannala, 2010), we performed a preliminary analysis estimating the two parameters under the MSC model with a given species phylogeny (with the topology obtained using the concatenated dataset) (Rannala & Yang, 2003). The suggested values were: θ = G(2, 600), τ = G(2,1000). The locus rate parameter that allows variable mutation rates among loci was estimated with a Dirichlet prior ($\alpha = 2$) and, since our dataset was only autosomal, the heredity parameter that allows θ to vary among loci was set as default. We ran each of the rjMCMC analyses twice to confirm consistency between runs, each run for 10^5 generations with 10% discarded as burn-in. We considered speciation probability values $\geq$ 0.95 as strong evidence for speciation.

We estimated divergence times with a species-tree approach using *BEAST (v.1.8.4; Heled & Drummond, 2010) with a dataset including the three lineages delimited within *P. minimus* (see Results) and the other *Spatalura* members (Table S1, see supplemental material online). We used jModelTest under the BIC to select the best model of nucleotide substitution for each gene. We set three calibration points for several nodes in the *Spatalura* clade as previously estimated in Garcia-Porta et al. (2017): (i) the divergence between *P. crucifer* and *P. somalicus* to 7.3–9 million years ago (Ma; normal distribution; mean 8, S.D. 2). (ii) the divergence between *P. collaris* and *P. carteri* to 9–13 Ma (normal distribution; mean 11, S.D. 2.5); and (iii) the divergence between *P. crucifer* and *P. somalicus* with *P. carteri* and *P. collaris* to 16–20 Ma (normal distribution; mean 18, S.D. 3). We analysed the data with the following partitions and relevant models (otherwise by default): *12S* (TrN + G), *ACM4* (HKY + I), *c-mos* (HKY with all equal frequencies), *MC1R* (HKY + I + G), Yule process tree model, random starting tree, base substitution parameter uniform (0–100), alpha prior uniform (0–10), uncorrelated relaxed clock for *12S* (uniform distribution; mean 0.01, 0–1) and strict clock for the nuclear genes (uniform distribution; mean 0.0001, 0–10). We performed three individual runs of 3×10^8 generations with sampling at intervals of every 3×10^4 generations. Convergence, posterior trace plots, effective sample size (>200), and burn-in were evaluated with Tracer. The tree runs were combined in LogCombiner discarding the first 10% as burn-in and the ultrametric tree was generated with TreeAnnotator.

Genetic diversity and demographic history analyses

We used DnaSP v.5.10.01 (Librado & Rozas, 2009) to estimate the genetic diversity within each marker (nuclear gene phased) for each clade: haplotype number, haplotype diversity, nucleotide diversity, haplotype polymorphisms, number of segregating sites, Tajima's D (Tajima, 1989) and Fu and Li's (including D and F; Fu & Li, 1993) tests, and calculate pairwise F_{ST} values between clades performing 10,000 permutations.

We investigated the demographic history and population size fluctuations of the three clades delimited within *P. minimus* (see Results) using a Bayesian skyline plot (BSP) generated in BEAST with the *12S* mitochondrial dataset. We performed the analyses with a rate extracted from the divergence time estimates described above (normal distribution; *12S*, mean 0.009657; S.D. 0.0005). Substitution models for each dataset were inferred using jModelTest2. We performed each analysis with the K80 substitution model, a strict clock prior and a Coalescent Bayesian Skyline tree prior; all other priors were by default. We performed five individual runs of 10^7 generations with sampling at intervals of every 10^3 generations and reconstructed the demographic history through time using Tracer.

Morphological specimens, examined characters, and multivariate analyses

We examined and included in the morphological analyses a total of 38 alcohol-preserved adult specimens of *P. minimus* from mainland Oman ($n = 23$) and Masirah Island ($n = 15$). All specimens were photographed using a Nikon 300 camera with a 60 mm macro-lens. A list of all studied voucher specimens with their coordinates is presented in Table S1 (see supplemental material online) and locations are shown in Fig. 1. All voucher specimens are from the Institute of Evolutionary Biology (IBE), Barcelona, Spain, the Natural History Museum

(BMNH), London, UK, and the Oman Natural History Museum (ONHM), Muscat, Oman. Variables for the morphological analyses were selected based on previous taxonomic studies of *Pristurus* (e.g., Arnold, 1977, 1993, 2009; Badiane et al., 2014; Garcia-Porta et al., 2017). Measurements were taken by the same author (P.M.) three times using a digital calliper (to the nearest 0.1 mm) and averages were used as the final value in all subsequent analyses. We measured the following morphometric characters: snout–vent length (SVL), distance from the tip of the snout to the cloaca; trunk length (TrL), distance between the fore and hind limb insertion points; head length (HL), taken axially from the tip of the snout to the anterior ear border; head height (HH), taken laterally at the anterior ear border; head width (HW), taken at the anterior ear border; humerus length (LHu), from the elbow to the insertion of the fore limb on the anterior part of body; ulna length (LUn), from the wrist to the elbow; femur length (LFe), from the knee to the insertion of the hind limb on the posterior side of body and tibia length (LTb), from the ankle to the knee. Tail length was not measured because many individuals had a regenerated tail or had lost it. In addition to those morphometric variables, we examined two pholidotic characters, counting from both the right and left sides: the number of upper labial scales (ULS) and the number of lower labial scales (LLS; anterior large scales only).

We performed statistical analyses with the specimens classified into the three bGMYC and BP&P clades (see Results) and with the specimens separated into two groups, mainland and Masirah Island. All variables were log-transformed to increase the homogeneity of variances. Sexual dimorphism was checked for size and shape using one-way ANOVAs. Regarding body size, we tested differences between groups using a one-way ANOVA on the log-transformed values of SVL. We also performed post-hoc t-tests when grouping specimens into three clades. In order to remove the effect of body size from the shape variables, we computed the residuals of each morphometric variable regressed against SVL using a linear regression. For these shape variables, we performed a principal component analysis (PCA) on the correlation matrix of the residuals to explore the shape variation of the groups. Then, we tested differences using MANOVA on the PCA scores from a number of components representing 80% of the total variance. We also analysed each component by performing one-way ANOVAs. In addition, the two pholidotic characters were tested using one-way ANOVA and t-tests. We performed all morphological analyses in R, using the packages 'Stats' (R Development Core Team, 2018) and 'ggbiplot' (Vu, 2011).

Species concept and ZooBank registration

In this manuscript we have adopted the General Lineage Species Concept (de Queiroz, 1998) that considers species as separately evolving meta-population lineages and treats this property as the single requisite for delimiting species. Other properties, such as phenetic distinguishability, reciprocal monophyly, and pre- and postzygotic reproductive isolation, are not part of the species concept but serve as important lines of evidence relevant to assess the separation of lineages and therefore to species delimitation (de Queiroz, 2007).

Results

Molecular analyses

The multilocus phylogenetic analyses using BI and ML methods comprised 72 *Pristurus* samples (Table S1, see supplemental material online), including the 55 samples of *P. minimus*, 16 samples of the new species described herein (the Masirah clade), and one specimen of *P. carteri* that was used to root the tree (Fig. 2.1). The phylogenetic analyses of the concatenated dataset resulted in largely similar topologies with high bootstrap support (ML) and posterior probabilities (BI) (Figs 2.1 and S1, see supplemental material online). The GMYC and bGMYC analyses based on the *12S* mitochondrial haplotypes dataset recovered five and three distinct entities, respectively (Fig. S2, see supplemental material online). The BP&P analyses based on the three phased nuclear loci support the three bGMYC distinct entities (Fig. 2.1). This result was consistent in all BP&P analyses carried out. The topology and the phylogenetic relationships of the BP&P species trees were identical to those of the phylogenetic tree based on the concatenated dataset.

In both ML and BI phylogenetic analyses, as well as in the bGMYC and BP&P delimitation analyses, three major well-supported clades were recovered: a Masirah clade from Masirah Island (16 specimens of the new species described herein), and two sister clades, clade A (35 specimens from mainland Oman, one from the UAE, and two specimens probably introduced from Masirah Island) and clade B (17 specimens from mainland Oman). The haplotype nuclear networks (Fig. 2.2) showed no allele sharing between the two mainland clades (clades A and B) and the Masirah clade from Masirah Island. In contrast, in all three nuclear networks there was allele sharing between the two mainland clades.

The uncorrected genetic distance in the *12S* mitochondrial fragment was $3 \pm 0.7\%$ between the two mainland clades A and B, $6.9 \pm 1.2\%$ between clade A and the

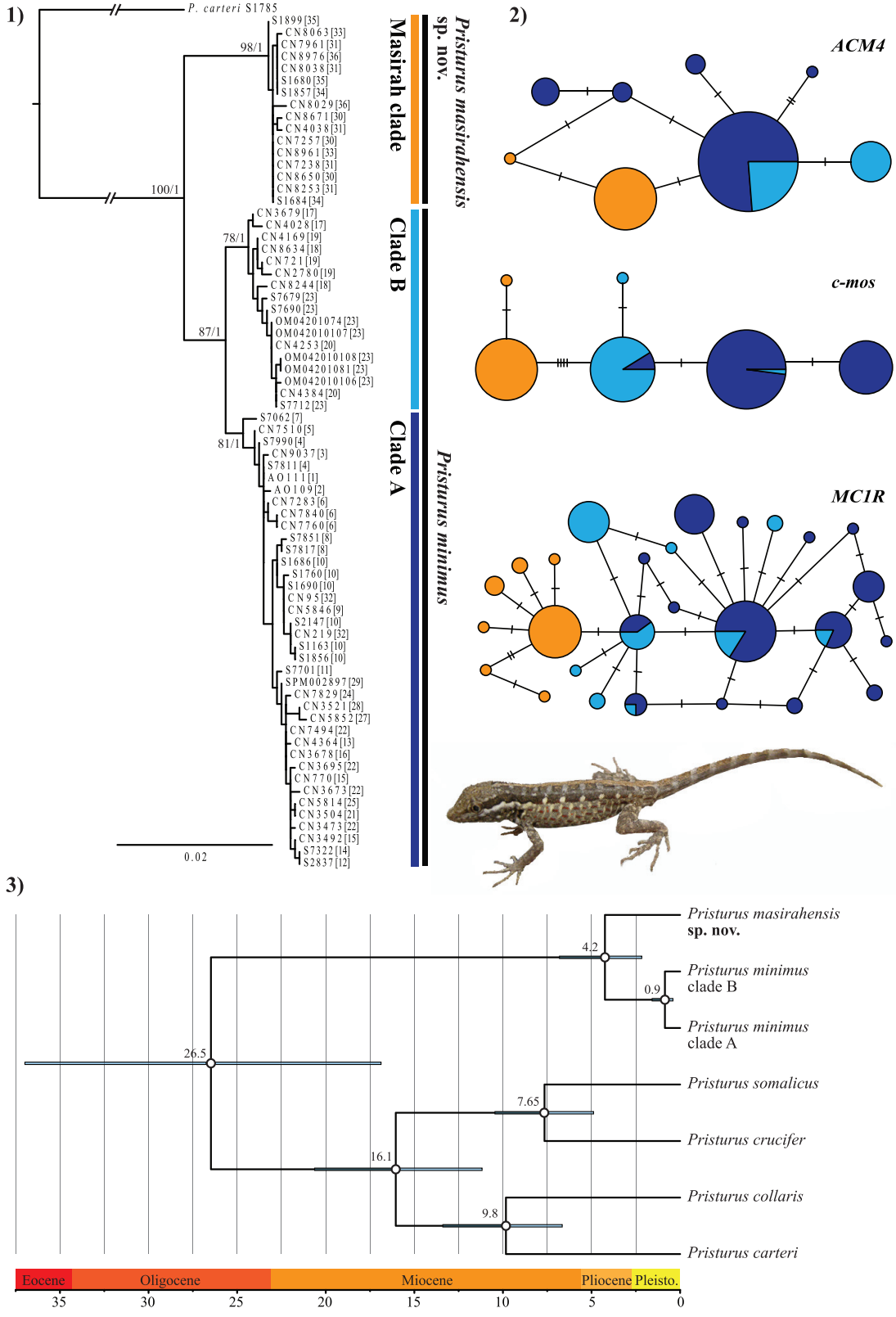

Fig. 2. Phylogenetic and network relationships of *Pristurus minimus* and *Pristurus masirahensis* sp. nov. Colours correspond to those in Figs 1–3. (2.1) Maximum likelihood phylogenetic tree reconstructed from the complete concatenated dataset (*12S*, *ACM4*, *c-mos*, *MC1R*). Support values are indicated near the nodes (ML bootstrap/Bayesian posterior probabilities). Sample codes correlate to specimens in Table S1 and localities (in brackets) are shown in Fig. 1. (2.2) Unrooted haplotype nuclear networks. Circle size is proportional to the number of alleles. (2.3) Time-calibrated species tree of species from the *Spatalura* clade. Mean age estimates are indicated near the nodes with bars representing the 95% highest posterior densities. White circles indicate nodes with posterior probability values ≥ 0.95.

Masirah clade, and 7.1 ± 1.2% between clade B and the Masirah clade. The level of genetic variability within clade A was 1.1 ± 0.3%, within clade B was 0.5 ± 0.2%, and within the Masirah clade was 0.3 ± 0.2%. The genetic distance between the mainland samples (clades A and B) and the Masirah Island ones (the Masirah clade; the new species described herein) was 6.9 ± 1.2% and the level of genetic variability within the mainland specimens was 1.8 ± 0.4%.

The dataset for the estimation of the divergence times using a species tree approach comprised 83 specimens: 71 of *P. minimus* and the new species described herein and 12 sequences of other species from the *Spatalura* clade (four of *P. carteri*, three of *P. collaris*, three of *P. crucifer*, and two of *P. somalicus*). The inferred ages from the phylogeny are shown in Fig. 2.3. The *Spatalura* clade started to diversify around 26.5 Ma (95% highest posterior densities [HPD]: 16.9–37). The split between *P. minimus* and the new species described herein started 4.2 Ma (95% HPD: 2.2–6.8), and the divergence between clades A and B of *P. minimus* occurred ∼0.9 Ma (95% HPD: 0.4–1.6).

In general, genetic diversity was low within each clade (Table S2, see supplemental material online). The neutrality tests performed were all statistically non-significant. These tests resulted mostly in negative values for the new species described herein and for the different markers contrasting values between the mainland clades A and B. The pairwise F_{ST} values between the mainland clades A and B and the Masirah clade were all high, indicating a relatively infrequent gene flow and great genetic differentiation. The F_{ST} results between the mainland clades A and B for *ACM4* and *MC1R* markers show relatively low values, though the value in the *c-mos* marker is higher.

Bayesian skyline plot analyses for the three clades (Fig. S3, see supplemental material online) showed a prolonged phase of demographic stability for clade B of *P. minimus* and for the new species described below. A demographic increase from ∼150,000 years ago occurred for clade A of *P. minimus* followed by stability at ∼50,000 years ago.

Multivariate analyses of the morphological data

The final dataset (Table S3, see supplemental material online) included 38 specimens divided according to the species delimitation analyses into three clusters: 17 specimens corresponding to clade A (12 males and five females), eight specimens corresponding to clade B (two males and six females), and 13 specimens to the Masirah clade (nine males and four females; described herein as a new species). Photographs of each specimen were uploaded to MorphoBank with related codes listed in Table S3 (see supplemental material online). Descriptive statistics for the nine morphometric and the two pholidotic variables (mean, standard deviation and range) for both sexes are presented in Tables 1 and S4 (see supplemental material online).

No sexual dimorphism is apparent in body size (SVL; $P = 0.44$) and body shape ($P > 0.08$ for all metric variables), thus we pooled together both sexes in the

Table 1. Descriptive statistics for all characters examined for males and females of *P. masirahensis* sp. nov. and *P. minimus*. Mean ± Standard Deviation (S.D.) and range (Min–Max) are given in millimetres for the morphometric variables, except for the pholidotic characters (ULS and LLS for the right and left sides). Abbreviations of characters as explained in the Materials and methods section. Taxon names follow the taxonomy proposed in this study.

	***P. masirahensis* sp. nov.**		***P. minimus***	
Variable	**Males ($n = 9$) Mean ± S.D. (Min–Max)**	**Females ($n = 4$) Mean ± S.D. (Min–Max)**	**Males ($n = 14$) Mean ± S.D. (Min–Max)**	**Females ($n = 11$) Mean ± S.D. (Min–Max)**
SVL	18.81 ± 1.78 (15.59–21.52)	19.38 ± 0.9 (18.45–20.25)	25.22 ± 2.81 (19.75–28.39)	24.33 ± 1.82 (21.42–27.16)
TrL	7.97 ± 1.05 (6.74–10.11)	8.38 ± 0.95 (7.09–9.37)	11.39 ± 1.43 (8.36–13.21)	11.09 ± 1.04 (9.15–12.54)
HL	4.59 ± 0.41 (4.11–5.21)	4.72 ± 0.34 (4.27–5.03)	6.17 ± 0.59 (5.03–6.84)	6 ± 0.36 (5.23–6.43)
HW	2.87 ± 0.28 (2.54–3.27)	2.87 ± 0.16 (2.64–3)	4.03 ± 0.44 (3.11–4.56)	3.75 ± 0.28 (3.35–4.2)
HH	2.57 ± 0.27 (2.08–2.9)	2.49 ± 0.22 (2.22–2.73)	3.37 ± 0.42 (2.41–3.86)	3.13 ± 0.39 (2.64–3.74)
LHu	2.73 ± 0.38 (2.25–3.3)	2.84 ± 0.5 (2.25–3.36)	3.6 ± 0.41 (3.1–4.35)	3.68 ± 0.47 (3.16–4.45)
LUn	2.71 ± 0.34 (2.02–3.11)	2.89 ± 0. 2 (2.68–3.13)	3.67 ± 0.49 (2.65–4.22)	3.53 ± 0.26 (3.02–4.11)
LFe	3.62 ± 0.44 (3.14–4.46)	3.68 ± 0.22 (3.43–3.97)	4.85 ± 0.5 (3.86–5.62)	4.57 ± 0.5 (3.74–5.33)
LTb	4.25 ± 0.6 (3.29–5.17)	4.34 ± 0.12 (4.17–4.45)	5.71 ± 0.95 (3.37–6.71)	5.46 ± 0.52 (4.73–6.57)
ULS (Right)	5.89 ± 0.33 (5–6)	6 ± 0	5.86 ± 0.36 (5–6)	6 ± 0
ULS (Left)	5.89 ± 0.33 (5–6)	6 ± 0	4.64 ± 0.5 (4–5)	4.82 ± 0.4 (4–5)
LLS (Right)	3.44 ± 0.53 (3–4)	4 ± 0	5.93 ± 0.27 (5–6)	6 ± 0
LLS (Left)	3.67 ± 0.5 (3–4)	4 ± 0	4.5 ± 0.52 (4–5)	4.64 ± 0.5 (4–5)

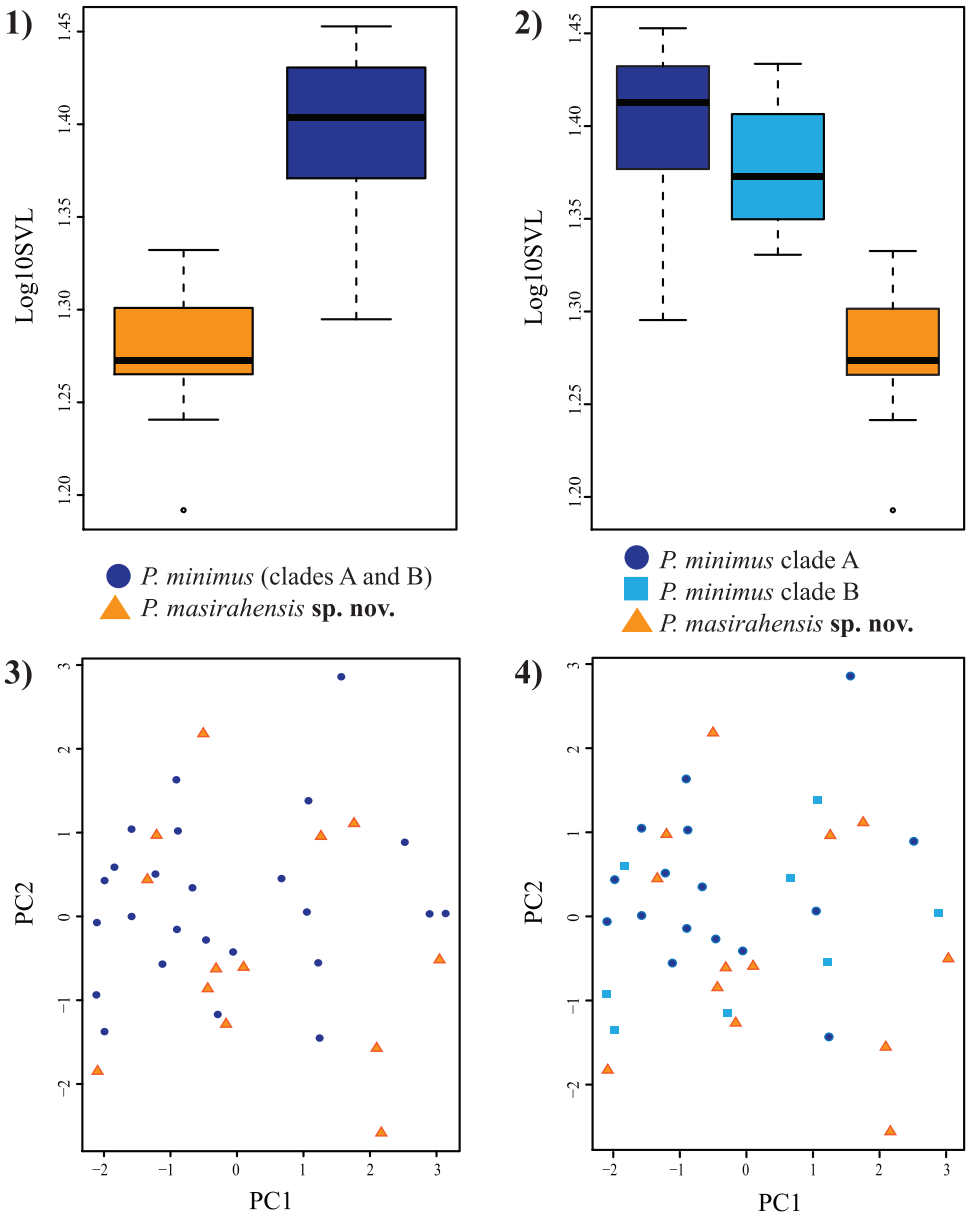

Fig. 3. Morphological comparisons. Results of the comparison between the two clades of *Pristurus minimus* (clade A, circle; clade B, square) and *Pristurus masirahensis* sp. nov. (triangle). Colours correspond to those in Figs 1, 2. (3.1, 3.2) Boxplots showing the $\log_{10}$SVL (body size) variation. (3.3, 3.4) The morphospaces obtained from the first two components of the PCA.

subsequent analyses. We found significant body size differences between specimens from mainland Arabia (clades A and B) and those from Masirah Island (the Masirah clade), the latter being significantly smaller ($F = 66.77$, d.f. $= 1$, $P < 0.0001$; Fig. 3.1). Among the three clades, the ANOVA analysis revealed significant body size differences ($F = 55.93$, d.f. $= 2$, $P < 0.0001$), and the t-tests detected these differences to originate between clades A and B and the Masirah clade ($P < 0.0001$ in both cases; Fig. 3.2).

For the comparison of body shape we retained the four first components, which explained 78% of the variance (the loadings of the PCA are presented in Table S5, see supplemental material online). Differences in body shape were not significant either between the mainland populations (clades A and B) and Masirah Island (the Masirah clade) or between the three clades (Wilk's $\lambda = 0.92$, $P = 0.59$ and Wilk's $\lambda = 0.74$, $P = 0.26$, respectively; Figs 3.3 and 3.4). Univariate tests performed on all the PCA scores were not

significant in most of the cases ($P > 0.24$ for all tests), except for the PC3 (accounting for 16% of the total variance), which was marginally significant ($P = 0.04$). Based on the current morphometric data, both the mainland populations and Masirah Island greatly overlap in their morphometric proportions.

Regarding the two pholidotic characters, we found significant differences between populations from the mainland (clades A and B) and Masirah Island (the Masirah clade) in the number of the lower labial scales (LLS) (right and left sides; $F = 46.28$, d.f. = 1, $P < 0.0001$ and $F = 22.74$, d.f. = 1, $P < 0.0001$, respectively). The same significant results were found when comparing between the three clades (right and left sides; $F = 23.03$, d.f. = 1, $P < 0.0001$ and $F = 14.54$, d.f. = 1, $P < 0.001$, respectively). The t-tests detected differences between each of the two mainland clades (clades A and B) with the Masirah clade for both sides ($P < 0.005$ in all four tests). Most of the specimens from the mainland have 4–5 lower labial scales (LLS) compared with the lower number of scales (3–4) found in the individuals from Masirah Island (see Tables 1 and S3–S4, see supplemental material online). Regarding the number of the upper labial scales (ULS), differences among groups (between the three clades and between mainland and Masirah Island) were not significant ($P > 0.3$ for all tests).

Taxonomic account

Given the genetic distinctiveness of the two main clades within *Pristurus minimus sensu lato* from mainland Arabia and from Masirah Island in the *12S* mitochondrial and three nuclear gene fragments analysed (Figs 2 and S1–S2; Tables S1–S2, see supplemental material online) and two morphological differences (see diagnosis below, Figs 3, 4; Tables S3–S4, see supplemental material online), we describe the unnamed populations from Masirah Island as a new species.

Despite the lack of genetic material in our analyses from the type locality of *P. minimus*, two specimens from localities 4 and 6 from clade A (specimens IBES7990 and CN7283, respectively) were collected from a close proximity to the type locality (see Fig. 1). These two specimens present a similar body size to the holotype of *P. minimus* (Arnold, 1977), which is significantly larger than the specimens of the new species described herein (Tables 1 and S3–S4, see supplemental material online). As a result of this body size differentiation and the vicinity of the localities from which genetic material was collected and analysed, we can confidently assign the mainland specimens to the species *P. minimus*.

Data for the morphological description of the new species was obtained from our morphological dataset (Table S3, see supplemental material online) and from the morphological information available within the original description of *P. minimus* (Arnold, 1977).

Family Sphaerodactylidae
Pristurus Rüppell, 1835

Pristurus minimus Arnold, 1977

(Figs 1–3, Figs S1–S3, see supplemental material online;
Table 1, Tables S1–S5, see supplemental material online)

Holotype. BMNH1969.312, adult female, Jazir coast (18.30 N, 56.30E approximately), Oman, collected by George Popov on 16 February 1968.

Paratypes. BMNH1969.313, adult female, same data as holotype; BMNH1975.1017–1025, two adult males, five adult females, two juveniles, between Bai (=Bawi) and Salalah, Oman, collected by Wilfred Thesiger in February 1947. Previous paratypes BMNH1971.1010–1012, BMNH1975.1033, BMNH1975.3086–87 collected from Masirah Island should be re-evaluated.

Other material examined. 55 specimens used for the genetic analyses, of which 25 adult voucher specimens used for both the genetic and morphological analyses; all specimens are listed in Tables S1 and S3.

Diagnosis. A small species of *Pristurus* from Oman, UAE, Saudi Arabia, and Yemen, belonging to the *Spatalura* clade *sensu* Arnold (2009), characterized by the combination of the following characters: (1) small size (up to 28.4 mm from snout to vent); (2) number of lower labial scales 4–5; (3) lateral down-growths of frontal bone not meeting on mid-line; (4) nasal process of premaxilla extending to about level of the anterior margins of orbits; (5) large area of contact between palatal sections of the maxillae behind the premaxilla; (6) low presacral vertebral count; (7) reduction of lateral arms of interclavicle; (8) nostril not bordered by rostral scale; (9) tails of males compressed, with sagittal ridges.

Distribution. *Pristurus minimus* is distributed in the south-east region of the Arabian Peninsula, mainly in north-east of the UAE, Oman, south-east Yemen, and Saudi Arabia. Two voucher specimens in our study were collected from Masirah Island; these specimens were most likely introduced to the island. It is usually found on soft ground, inhabiting sandy areas with shrubby vegetation.

Pristurus masirahensis sp. nov.

(Figs 1–4, Figs S1–S3, see supplemental material online;
Table 1, Tables S1–S5, see supplemental material online)

urn:lsid:zoobank.org:pub:DB0658D5-7F68-4E66-885F-75E27F9CD512

Pristurus minimus Arnold (1977): 93 (part.), Arnold (1980): 287 (part.); Sindaco and Jeremčenko (2008): 121 (part.); Badiane et al. (2014): 40 (part.); Gardner (2013): 174 (part.); Carranza et al. (2018): 60 (S2 Appendix, see supplemental material online) (part.).

Holotype. NHMUK2019.2894 (sample code CN8253), adult male, from 1 km north-east of Urf, Masirah Island, Oman (20. 25509 N, 58. 74441E WGS84; locality 31 in Fig. 1), collected by Salvador Carranza on 13 August 2017.

Paratypes. IBECN4038, IBECN7238, two adult females, and IBECN7961, IBECN8038, two adult males, same data as the holotype; IBECN7257 and IBECN8650, two adult males, from the southern edge of Masirah Island, Oman, collected by Salvador Carranza on 13 August 2017; IBECN8063 and IBECN8961, two adult males, from 3.5 km west of Sur Masirah, Masirah Island, Oman, collected by Salvador Carranza on 13 and 14 August 2017; IBECN8029 and IBECN8976, two adult females, from 1 km north-east of Dafiyat, Masirah Island, Oman, collected by Salvador Carranza on 11 August 2017. ONHM4238 (sample code S1857), adult male, from Maghilah, Masirah Island, Oman, collected by Nicolas Arnold, Salim Alrabei, and Salvador Carranza on 27 October 2008.

Other material examined. Four specimens used for the genetic analyses, of which one voucher specimen was used for both the genetic and morphological analyses; all specimens are listed in Tables S1 and S3.

Etymology. The species epithet '*masirahensis*' is an adjective that refers to the distribution range of the species, restricted to Masirah Island, Oman.

Diagnosis. A new species of *Pristurus* endemic to Masirah Island, belonging to the *Spatalura clade sensu* Arnold (2009), characterized by the combination of the following characters: (1) small size (up to 21.5 mm from snout to vent); (2) number of lower labial scales 3–4; (3) lateral down-growths of frontal bone not meeting on mid-line; (4) nasal process of premaxilla extending to about level of the anterior margins of orbits; (5) large area of contact between palatal sections of the maxillae behind the premaxilla; (6) low presacral vertebral count; (7) reduction of lateral arms of interclavicle; (8) nostril not bordered by rostral scale; (9) tails of males compressed, with sagittal ridges.

Differential diagnosis. *Pristurus masirahensis* sp. nov. differs from *P. minimus* mainly in its smaller size (SVL max. 21.5 mm, compared with max. 28.4 mm) and in having fewer lower labial scales (3–4 *vs* 4–5). It further differs by a genetic distance of 7% in the *12S* mitochondrial gene and in the presence of private alleles in the *ACM4*, *c-mos*, and *MC1R* nuclear genes analysed (Fig. 2.2). It is distinguished from the sympatric *P. carteri* by its smaller size, fewer lower labials, and different colour pattern. It is distinguished from the morphologically similar *P. crucifer* by its smaller size, upper profile of head less bulbous, nostril nearly always situated between three scales (instead of within one or between two as is usual in *P. crucifer*), fewer coarser scales across mid-orbits on upper surface of head, flanks often have extensive dark grey pigment reducing the pale ground colour to more or less vertical wavy lines, low crest on midline of tail made up of two longitudinal rows of scales instead of one row. It is distinguished from *P. rupestris sensu lato* which was recently found on Masirah Island (S. Carranza pers. comm.) by its smaller size, colour pattern, nostril not in contact with rostral scale, tail not laterally compressed and with no pronounced dorsal fringe of elongated scales on midline (mainly in males).

Description of the holotype. NHMUK2019.2894 (sample code CN8253) (Fig. 4). Adult male. Complete specimen with the tip of the tongue missing (used for DNA extraction) and tail detached. Data on nine morphometric and two pholidotic variables (see Materials and methods) are provided in Table S3 (see supplemental material online). SVL 17.44 mm, head length 25.5% of SVL, and head width 60% of head length, tail not regenerated. Moderately built with head and body only slightly depressed; limbs and tail not especially slender. Head is slightly depressed and does not rise very steeply in profile. Rostral scale hexagonal with shortest sides dorsal and lateral. Nostril separated from the rostral and situated between three scales: a wide supranasal extending to the midline margin, a small upper postnasal and a large lower postnasal extending laterally along the lower edge. Supranasals are separated by two scales. Scales on snout coarse, polygonal and pointed upwards. About eight scales in a straight line from the lower postnasal to the anterior edge of the orbit. Scales on snout, anterior to eyes, are larger than those on top of head. Around 22 scales across mid-orbital region. Palpebral fold edged anteriorly with large scales but not projecting much dorsally and not edged with pointed (ciliate) scales. Ear

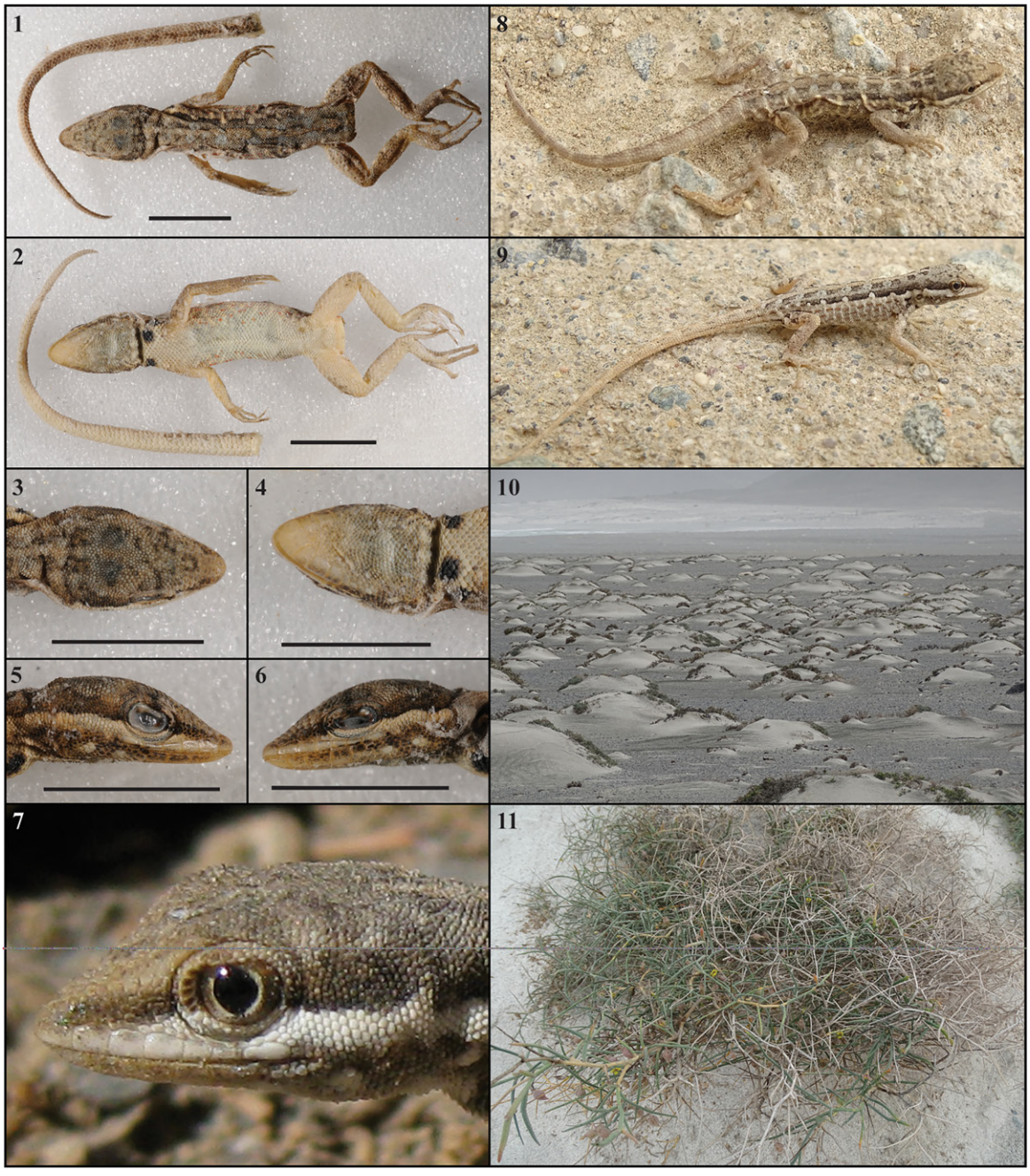

Fig. 4. General appearance and habitat of *Pristurus masirahensis* sp. nov. (4.1) Holotype NHMUK2019.2894, habitus, dorsal view. (4.2) Holotype NHMUK2019.2894, habitus, ventral view. (4.3) Holotype NHMUK2019.2894, head, dorsal view. (4.4) Holotype NHMUK2019.2894, head, ventral view. (4.5) Holotype NHMUK2019.2894, head, right view. (4.6) Holotype NHMUK2019.2894, head, left view. (4.7) Paratype ONHM4238, adult male, head, lateral view. (4.8) Holotype NHMUK2019.2894, adult male. (4.9) Paratype IBECN7238, adult female. (4.10) Habitat, 1 km north-east of Urf (locality 31), Masirah Island. (4.11) The plant, *Crotalaria aegyptiaca* (family Fabaceae), found in the habitat. Scale bars = 5 mm. Photos by Salvador Carranza.

opening round, slightly narrow. Upper labials (right/left) 6/6. Lower labials (right/left) 3/4, the fourth decreasing in size from the three large anterior scales. Three to four enlarged scales running backwards along the medial borders of the third lower labials to end at about the level of the angle of the mouth. Mental large, wedge-shaped, rounded posteriorly. Mental bordered posteriorly by three gular scales. Gulars small, rather pointed posteriorly, becoming increasingly imbricate on throat.

Dorsal scales on body small, polygonal and homogeneous, slightly pointed posteriorly and imbricate.

Ventrals flat and distinctly imbricate, the largest at mid-body double the diameter of corresponding dorsals, each about as long as broad. Scales in interfemoral area smaller than the ventrals.

Scales on dorsal and anterior surface of the fore limbs large, flat and imbricate, fairly pointed. Scales beneath the upper fore limbs granular and smaller than ventral body scales; those beneath lower fore limbs large, flat, imbricate and pointed, larger than ventral body scales. Claws relatively shallow and weakly recurved. Scales on dorsal and anterior surface of hind limbs large, flat and imbricate, fairly pointed. Scales beneath the upper hind limbs granular and smaller than ventral body scales, those beneath lower hind limbs large, flat, imbricate and pointed, larger than ventral body scales.

Tail relatively short and robust, more or less cylindrical, with a slight groove along each side. No ridges of elongate scales present, but very low crest on midline of tail is made up of two longitudinal rows of scales and a row of scales on lower mid-line slightly enlarged and weakly keeled. Tail scales large, flat and imbricate, pointed posteriorly; dorsals considerably larger than those on body, with a single apical pit; ventrals bigger still, some with two apical pits.

Colouration in alcohol is light brown above; midline of back paler and slightly greyish, bordered on each side by a wide darker brown-grey strip, those are bordered on each side by black colouration. Nine pairs of light grey blotches cross the dorsum running from neck to base of tail, located on each lateral dark strip. The most lateral black lines are darker and run from the nostril through the eye and then dorso-laterally on the body. This fades in the sacral region and is partly interrupted by a series of whitish strips and spots of which there are six on each side of the body between the fore and hind limbs; this white strip begins from the second upper labial. A black blotch present on the neck flanks on each side, behind the ear opening. Head is light brown with dark irregular marks, and two dark blotched behind the eyes. Flanks with greyish-brown shades, with irregular light bands and rows of small, elongate red dots that continue towards the ventrals. Ventral colouration is whitish; the gulars have a darker shade, pale blue-grey pigment. Two black blotches present on each side of neck just in front of forelimb insertion. Limbs light brown with irregular dark brown markings above; ventrals are white. Tail lighter than the dorsals, pale grey-brown above with weak, light, narrow cross-bars that form a continuation from the dorsal grey blotches; a darker midline strip runs along the tail on two scales.

Variation. Data on nine morphometric and two pholidotic variables (see Materials and methods) for all 11 paratypes (see above) are provided in Table S3. Largest male 21.52 mm snout to vent; largest female 20.25 mm. All paratypes have broken tails. Paratypes IBECN2757 and IBECN7961, two females, have regenerated tails; paratypes IBECN7961, IBECN8038, ONHM4238, three males, have cut tails; paratypes IBECN8029, IBECN8063, IBECN8961 and IBECN8976, four males, do not have tails.

Distribution and ecology. *Pristurus masirahensis* sp. nov. is endemic to Masirah Island, Oman. It has been found on flat sandy areas with few stones and scattered low vegetation, mainly in the coastal plains and in suitable habitats inland. The species has been observed underneath shrubs as *Crotalaria aegyptiaca* (family Fabaceae) (Figs 4.10–4.11).

Discussion

In this study, we uncovered an old diversification event that has resulted in a case of island endemicity. We used an integrative approach applying phylogenetic and species delimitation methods with morphological comparisons to assess the intraspecific diversity of the smallest *Pristurus* species distributed in mainland Arabia and Masirah Island. We discovered two morphologically and ecologically similar small-sized gecko species that occur in Arabia, one mainly on the mainland, *P. minimus*, and another endemic to Masirah Island, *P. masirahensis* sp. nov. According to our phylogenetic analyses, the genetic distinctiveness of *P. masirahensis* sp. nov. is evident at both the mitochondrial and nuclear levels, with private alleles in the three nuclear genes analysed, suggesting reproductive isolation from the mainland populations. Interestingly, two specimens from clade A, IBECN95 and IBECN219, which genetically and morphologically belong to *P. minimus* were collected from Masirah Island. The high genetic similarity of these individuals to the other specimens of the mainland clade and the genetic structure uncovered may suggest a plausible scenario in which they probably spread to the island by human-mediated dispersal (e.g., building material and other goods arriving by boat) rather than natural colonization.

With a maximum recorded SVL size of 21.5 mm, *Pristurus masirahensis* sp. nov. is the smallest Arabian vertebrate, significantly smaller than any Arabian amphibian, fish, bird, and mammal species, and smaller than any other minute Arabian reptile, such as *P. minimus* (this study), *P. rupestris* (Badiane et al., 2014; Garcia-Porta et al., 2017), *Hemidactylus minutus* (Vasconcelos & Carranza, 2014), and *H. pumilio* (Gómez-Díaz et al., 2012). In fact, *Pristurus masirahensis* sp. nov. is one of the smallest lizards in the world,

together with the geckos *Sphaerodactylus ariasae* and *S. parthenopion*, with a maximum SVL of 18 mm (Hedges & Thomas, 2001), and several species of chameleons of the genus *Brookesia* from Madagascar, including *B. micra*, with a maximum SVL of 19.9 mm (Glaw, Köhler, Townsend, & Vences, 2012).

Body sizes of animals on islands often differ substantially from those of their mainland conspecifics. It is well documented that after island colonization, the new arrivals often undergo evolutionary changes as they encounter new niches and are not subjected to the same high levels of interspecific competition and predation that usually occur in their previous source population (Harmon & Gibson, 2006; Losos & Mahler, 2010; Schluter, 2000; Yoder et al., 2010). Thus, insular taxa can experience great levels of phenotypic diversification, developing distinctive adaptations to their new habitats and community structures (Schluter, 1988). Indeed, body size is most frequently the first morphological trait to be modified after island colonization, as demonstrated by many evolutionary studies (Losos, 2009; Price, Helbig, & Richman, 1997; Raia & Meiri, 2006; Williams, 1972). It has been shown that lizards on islands may evolve large or small body sizes, due to a combination of adaptive and non-adaptive factors, such as character release, resource limitation, increased population densities, or just random genetic drift (see Kolbe, Leal, Schoener, Spiller, & Losos, 2012; Meiri, 2007, 2008 for references). In our study, the morphological differentiation between the two species mainly relies on body size, without significant differences in body shape, with the island endemic, *P. masirahensis* sp. nov., being significantly smaller than its mainland sister taxon. As an arid island, Masirah Island has limited food resources, and this resource limitation may drive a decrease in body size. Therefore, one possible explanation of our results is an association between the smaller body size and a regime of reduced resource availability. Another, not mutually exclusive, hypothesis is that the smaller size of *P. masirahensis* sp. nov. was caused by reduced competition, as all other lizards distributed on Masirah Island (e.g., *P. carteri*) are larger. The smaller size of *P. masirahensis* sp. nov. might also be the result of a random process (genetic drift) due to a founder effect by small-sized first colonizers; a trait that was later fixed in the population.

According to the distribution range of *Pristurus minimus* and *P. masirahensis* sp. nov. (see Fig. 1), the only physical barrier between the two species is the Arabian Sea. *Pristurus masirahensis* sp. nov. is geographically isolated, endemic to Masirah Island and genetically very distinct, suggesting a process of allopatric speciation through geographic isolation. The two species are estimated to have diverged ~4.2 Ma, during the Pliocene, thus providing enough time to accumulate changes which led to reproductive isolation. This timeframe has also been suggested in numerous studies on Arabian reptiles (e.g., Carranza et al., 2016; Carranza & Arnold, 2012; Simó-Riudalbas et al., 2017, 2018; Tamar et al., 2016a, 2016b, 2018, 2019). Interestingly, the only other gecko species endemic to Masirah Island, *Hemidactylus masirahensis*, diverged from its sister taxon *H. inexpectatus* about 4.4 and 4.8 Ma (Carranza & Arnold, 2012; Šmíd et al., 2013a, respectively). However, in contrast to the phenotypical similarity between the two *Pristurus* species, *H. masirahensis* and *H. inexpectatus* are morphologically distinct and easily diagnosable (Carranza & Arnold, 2012). The Pliocene colonization of the ancestral populations of *P. masirahensis* sp. nov. and *Hemidactylus masirahensis* on Masirah Island is hard to interpret, since the area lacks adequate geological and climatic data. Palaeoclimate reconstructions suggest that the Indian Ocean monsoon cycles shifted abruptly during the Pliocene (see Fleitmann et al., 2007; Gupta, Singh, Joseph, & Thomas, 2004; and references therein). As a result of the changing precipitation patterns, changes in wind direction and strength, and monsoon-driven upwelling, major environmental changes have occurred affecting the local marine and terrestrial fauna and flora in the Arabian Sea. We may hypothesize that these climatic changes have played a role in the colonization of the ancestral populations of *P. masirahensis* sp. nov. and *Hemidactylus masirahensis* on Masirah Island, though with the data at hand we cannot conclude so with certainty.

The intraspecific divergence between the two *P. minimus* clades occurred recently, during the Pleistocene, around 0.9 Ma. One of them (clade B) is restricted to the coastal plains of north-eastern Oman. The presence of allele sharing between these two clades may stem from the presence of gene flow or alternatively, due to their recent divergence. We thus should conservatively consider them as two distinct evolutionary units that necessitate further investigation in the future. This genetic structure exemplifies the importance of broad geographic sampling in order to understand evolutionary processes.

According to the IUCN Red List of Threatened Species, *Pristurus minimus* is listed as Least Concern (Burriel-Carranza et al., 2019; Carranza et al., 2018; Sindaco, 2012) as it is locally abundant and not subjected to any threats within its range. Our systematic revision should have conservation implications, considering the endemicity of the new species to Masirah Island. The new species' conservation status should

therefore be evaluated, investigating and taking into account some unknown parameters, such as its population trends. Regarding *Pristurus minimus*, which is abundant mainly in mainland Oman, this revision might not affect its status as Least Concern, yet it still should be properly re-assessed.

Acknowledgements

We wish to thank Ali Alghafri, Sultan Khalifa, Hamed Al Furkani, Margarita Metallinou, Jiri Šmíd, Raquel Vasconcelos, Philip de Pous, and Felix Amat for assisting in sample collection in the field. Special thanks are due to Saleh Al Saadi, Salim Bait Bilal, Iman Sulaiman Alazri, Ahmed Said Al Shukaili, Mohammed Al Shariani, Ali Al Kiyumi, Suleiman Nasser Al Akhzami, and the other members of the Nature Conservation Department of the Ministry of Environment and Climate, Oman for their help and support. Specimens were collected and manipulated with the authorization and under control and permission of the government of Oman (Ministry of Environment and Climate Affairs, MECA). All the necessary collecting and export permits for this study in Oman were issued by the Nature Conservation Department of the Ministry of Environment and Climate Affairs, Oman (Refs: 08/2005; 16/2008; 38/2010; 12/2011; 13/2013; 21/2013; 37/2014; 31/2016; 6210/10/21).

Funding

This work was supported by the Ministerio de Economía y Competitividad, Spain (co-funded by FEDER) under [Grant number CGL2012-36970], [Grant number CGL2015-70390-P]; Ministry of Environment and Climate Affairs under [Grant number 22412027]; Secretaria d'Universitats i Recerca del Departament d'Economia i Coneixement de la Generalitat de Catalunya under [Grant number 2017-SGR-00991].

Supplemental data

Supplemental data for this article can be accessed here: https://dx.doi.org/10.1080/14772000.2019.1614694

Disclosure statement

No potential conflict of interest was reported by the author(s).

Funding

This work was supported by the Ministerio de Economía y Competitividad, Spain (co-funded by FEDER) under [Grant number CGL2012-36970], [Grant number CGL2015-70390-P]; Ministry of Environment and Climate Affairs under [Grant number 22412027]; Secretaria d'Universitats i Recerca del Departament d'Economia i Coneixement de la Generalitat de Catalunya under [Grant number 2017-SGR-00991].

References

Arnold, E. N. (1977). The scientific results of the Oman flora and fauna survey 1975. Little-known geckos (Reptilia: Gekkonidae) from Arabia with descriptions of two new species from the Sultanate of Oman. *Journal of Oman Studies, Special Report*, *1*, 81–110.

Arnold, E. N. (1980). Reptiles and amphibians of Dhofar, Southern Arabia. *Journal of Oman Studies, Special Report*, *2*, 273–332.

Arnold, E. N. (1993). Historical changes in the ecology and behaviour of semaphore geckos (*Pristurus*, Gekkonidae) and their relatives. *Journal of Zoology*, *229*, 353–384. doi: 10.1111/j.1469-7998.1993.tb02642.x

Arnold, E. N. (2009). Relationships, evolution and biogeography of Semaphore geckos, *Pristurus* (Squamata, Sphaerodactylidae) based on morphology. *Zootaxa*, *2060*, 1–21.

Badiane, A., Garcia-Porta, J., Červenka, J. A. N., Kratochvíl, L., Sindaco, R., Robinson, M. D., … Carranza, S. (2014). Phylogenetic relationships of Semaphore geckos (Squamata: Sphaerodactylidae: *Pristurus*) with an assessment of the taxonomy of *Pristurus rupestris*. *Zootaxa*, *3835*, 33–58. doi: 10.11646/zootaxa.3835.1.2

Bruen, T. C., Hervé, P., & Bryant, D. (2006). A simple and robust statistical test for detecting the presence of recombination. *Genetics*, *172*, 2665–2681. doi:10.1534/genetics.105.048975

Burriel-Carranza, B., Tarroso, P., Els, J., Gardner, A., Soorae, P., Mohammed, A. A., … Carranza, S. (2019). An integrative assessment of the diversity, phylogeny, distribution, and conservation of the terrestrial reptiles (Sauropsida, Squamata) of the United Arab Emirates. *Public Library of Science One*, *14*, e0216273. doi:10.1371/journal.pone.0216273

Carranza, S., & Arnold, E. N. (2012). A review of the geckos of the genus *Hemidactylus* (Squamata: Gekkonidae) from Oman based on morphology, mitochondrial and nuclear data, with descriptions of eight new species. *Zootaxa*, *3378*, 1–95.

Carranza, S., Simó-Riudalbas, M., Jayasinghe, S., Wilms, T., & Els, J. (2016). Microendemicity in the northern Hajar Mountains of Oman and the United Arab Emirates with the description of two new species of geckos of the genus *Asaccus* (Squamata: Phyllodactylidae). *PeerJ*, *4*, e2371. doi: 10.7717/peerj.2371

Carranza, S., Xipell, M., Tarroso, P., Gardner, A., Arnold, E. N., Robinson, M. D., … Al Akhzami, S. N. (2018). Diversity, distribution and conservation of the terrestrial reptiles of Oman (Sauropsida, Squamata). *Public Library of Science One*, *13*, e0190389. doi:10.1371/journal.pone.0190389

Clement, M., Posada, D., & Crandall, K. A. (2000). TCS: A computer program to estimate gene genealogies. *Molecular*

Ecology, *9*, 1657–1660. doi:10.1046/j.1365-294x.2000.01020.x

de Pous, P., Machado, L., Metallinou, M., Červenka, J., Kratochvíl, L., Paschou, N., … Carranza, S. (2016). Taxonomy and biogeography of *Bunopus spatalurus* (Reptilia; Gekkonidae) from the Arabian Peninsula. *Journal of Zoological Systematics and Evolutionary Research*, *54*, 67–81. doi:10.1111/jzs.12107

de Queiroz, K. (1998). The general lineage concept of species, species criteria, and the process of speciation: A conceptual unification and terminological recommendations. In D. J. Howard & S. H. Berlocher (Eds.), *Endless forms: Species and speciation* (pp. 57–75). Oxford: Oxford University Press.

de Queiroz, K. (2007). Species concepts and species delimitation. *Systematic Biology*, *56*, 879–886. doi:10.1080/10635150701701083

Drummond, A. J., Suchard, M. A., Xie, D., & Rambaut, A. (2012). Bayesian phylogenetics with BEAUti and the BEAST 1.7. *Molecular Biology and Evolution*, *29*, 1969–1973. doi:10.1093/molbev/mss075

Edgell, H. S. (2006). *Arabian deserts: Nature, origin and evolution*. Dordrecht: Springer.

Ezard, T., Fujisawa, T., & Barraclough, T. G. (2009). Splits: Species' limits by threshold statistics. *R package version*, 1.0-19/r51.

Fleitmann, D., Burns, S. J., Mangini, A., Mudelsee, M., Kramers, J., Villa, I., … Matter, A. (2007). Holocene ITCZ and Indian monsoon dynamics recorded in stalagmites from Oman and Yemen (Socotra). *Quaternary Science Reviews*, *26*, 170–188. doi:10.1016/j.quascirev.2006.04.012

Flot, J. F. (2010). Seqphase: A web tool for interconverting phase input/output files and FASTA sequence alignments. *Molecular Ecology Resources*, *10*, 162–166. doi:10.1111/j.1755-0998.2009.02732.x

Fu, Y. X., & Li, W. H. (1993). Statistical tests of neutrality of mutations. *Genetics*, *133*, 693–709.

Fujisawa, T., & Barraclough, T. G. (2013). Delimiting species using single-locus data and the Generalized Mixed Yule Coalescent approach: A revised method and evaluation on simulated data sets. *Systematic Biology*, *62*, 707–724. doi:10.1093/sysbio/syt033

Fujita, M. K., & Papenfuss, T. J. (2011). Molecular systematics of *Stenodactylus* (Gekkonidae), an Afro-Arabian gecko species complex. *Molecular Phylogenetics and Evolution*, *58*, 71–75. doi:10.1016/j.ympev.2010.10.014

Gallagher, M. D., & Arnold, E. N. (1988). Reptiles and amphibians from the Wahiba Sands, Oman. *Journal of Oman Studies, Special Report*, *3*, 405–413.

Garcia-Porta, J., Simó-Riudalbas, M., Robinson, M., & Carranza, S. (2017). Diversification in arid mountains: Biogeography and cryptic diversity of *Pristurus rupestris rupestris* in Arabia. *Journal of Biogeography*, *44*, 1694–1704. doi:10.1111/jbi.12929

Gardner, A. S. (2013). *The amphibians and reptiles of Oman and the UAE*. Frankfurt am Main: Chimaira.

Glaw, F., Köhler, J., Townsend, T. M., & Vences, M. (2012). Rivaling the world's smallest reptiles: Discovery of miniaturized and microendemic new species of leaf chameleons (*Brookesia*) from northern Madagascar. *Public Library of Science One*, *7*, e31314. doi:10.1371/journal.pone.0031314

Gómez-Díaz, E., Sindaco, R., Pupin, F., Fasola, M., & Carranza, S. (2012). Origin and in situ diversification in *Hemidactylus* geckos of the Socotra Archipelago. *Molecular Ecology*, *21*, 4074–4092. doi:10.1111/j.1365-294X.2012.05672.x

Gupta, A. K., Singh, R. K., Joseph, S., & Thomas, E. (2004). Indian Ocean high-productivity event (10–8 Ma): Linked to global cooling or to the initiation of the Indian monsoons? *Geology*, *32*, 753–756. doi:10.1130/G20662.1

Harmon, L., & Gibson, R. (2006). Multivariate phenotypic evolution among island and mainland populations of the ornate day gecko, *Phelsuma ornata*. *Evolution*, *60*, 2622–2632. doi:10.1111/j.0014-3820.2006.tb01894.x

Hedges, S. B., & Thomas, R. (2001). At the lower size limit in Amniote vertebrates: A new diminutive lizard from the West Indies. *Caribbean Journal of Sciences*, *37*, 168–173.

Heled, J., & Drummond, A. J. (2010). Bayesian inference of species trees from multilocus data. *Molecular Biology and Evolution*, *27*, 570–580. doi:10.1093/molbev/msp274

Huson, D. H., & Bryant, D. (2006). Application of phylogenetic networks in evolutionary studies. *Molecular Biology and Evolution*, *23*, 254–267. doi:10.1093/molbev/msj030

Immenhauser, A. (1996). Cretaceous sedimentary rocks on the Masirah Ophiolite Sultanate of Oman); evidence for an unusual bathymetric history. *Journal of the Geological Society London*, *153*, 539–551. doi:10.1144/gsjgs.153.4.0539

Katoh, K., & Standley, D. M. (2013). MAFFT multiple sequence alignment software version 7: Improvements in performance and usability. *Molecular Biology and Evolution*, *30*, 772–780. doi:10.1093/molbev/mst010

Kolbe, J. J., Leal, M., Schoener, T. W., Spiller, D. A., & Losos, J. B. (2012). Founder effects persist despite adaptive differentiation: A field experiment with lizards. *Science*, *335*, 1086–1089. doi:10.1126/science.1209566

Kumar, S., Stecher, G., & Tamura, K. (2016). MEGA7: Molecular evolutionary genetics analysis version 7.0 for bigger datasets. *Molecular Biology and Evolution*, *33*, 1870–1874. doi:10.1093/molbev/msw054

Lanfear, R., Frandsen, P. B., Wright, A. M., Senfeld, T., & Calcott, B. (2016). PartitionFinder 2: New methods for selecting partitioned models of evolution for molecular and morphological phylogenetic analyses. *Molecular Biology and Evolution*, *34*, 772–773. doi:10.1093/molbev/msw260

Leigh, J. W., & Bryant, D. (2015). PopART: Full feature software for haplotype network construction. *Methods in Ecology and Evolution*, *6*, 1110–1116. doi:10.1111/2041-210X.12410

Librado, P., & Rozas, J. (2009). DnaSP v5: A software for comprehensive analysis of DNA polymorphism data. *Bioinformatics*, *25*, 1451–1452. doi:10.1093/bioinformatics/btp187

Losos, J. B. (2009). *Lizards in an evolutionary tree: Ecology and adaptive radiation of anoles*. Berkeley: University of California Press.

Losos, J. B., & Mahler, D. L. (2010). Adaptive radiation: The interaction of ecological opportunity, adaptation, and speciation. In M. A. Bell, D. J. Futuyma, W. F. Eanes, & J. S. Levinton (Eds.), *Evolution since Darwin: The first years* (pp. 381–420). Sunderland, Massachusetts: Sinauer Associates.

Meiri, S. (2007). Size evolution in island lizards. *Global Ecology and Biogeography*, *16*, 702–708. doi:10.1111/j.1466-8238.2007.00327.x

Meiri, S. (2008). Evolution and ecology of lizard body sizes. *Global Ecology and Biogeography*, *17*, 724–734. doi:10.1111/j.1466-8238.2008.00414.x

Metallinou, M., Arnold, E. N., Crochet, P. A., Geniez, P., Brito, J. C., Lymberakis, P., … Carranza, S. (2012). Conquering the Sahara and Arabian deserts: Systematics and biogeography of *Stenodactylus* geckos (Reptilia: Gekkonidae). *BioMed Central Evolutionary Biology*, *12*, 258. doi:10.1186/1471-2148-12-258

Metallinou, M., & Carranza, S. (2013). New species of *Stenodactylus* (Squamata: Gekkonidae) from the Sharqiyah Sands in northeastern Oman. *Zootaxa*, *3745*, 449–468. doi:10.11646/zootaxa.3745.4.3

Metallinou, M., & Crochet, P.-A. (2013). Nomenclature of African species of the genus *Stenodactylus* (Squamata: Gekkonidae). *Zootaxa*, *3691*, 365–376. doi:10.11646/zootaxa.3691.3.5

Moseley, F. (1990). The structure of Masirah Island, Oman. *Geological Society, London, Special Publications*, *49*, 665–671. doi:10.1144/GSL.SP.1992.049.01.40

Moseley, F. (1969). The upper cretaceous ophiolite complex of Masirah Island, Oman. *Geological Journal*, *6*, 293–306. doi:10.1002/gj.3350060211

Moseley, F., & Abbotts, I. L. (1979). The ophiolite melange of Masirah, Oman. *Journal of the Geological Society, London*, *136*, 713–724. doi:10.1144/gsjgs.136.6.0713

Papenfuss, T. J., Jackman, T., Bauer, A., Stuart, B. L., Robinson, M. D., & Parham, J. F. (2009). Phylogenetic relationships among species in the sphaerodactylid lizard genus *Pristurus*. *Proceedings of California Academy of Sciences*, *60*, 675–681.

Pons, J., Barraclough, T. G., Gomez-Zurita, J., Cardoso, A., Duran, D. P., Hazell, S., … Vogler, A. P. (2006). Sequence-based species delimitation for the DNA taxonomy of undescribed insects. *Systematic Biology*, *55*, 595–609. doi:10.1080/10635150600852011

Price, T. D., Helbig, A. J., & Richman, A. D. (1997). Evolution of breeding distributions in the Old World leaf warblers (genus *Phylloscopus*). *Evolution*, *51*, 552–561.

R Development Core Team. (2018). *R: A language and environment for statistical computing*. Vienna: The R Foundation for Statistical Computing. ISBN: 3-900051-07-0. Retrieved from http://www.R-project.org/ (accessed 30 April 2019).

Raia, P., & Meiri, S. (2006). The island rule in large mammals: Paleontology meets ecology. *Evolution*, *60*, 1731–1742. doi:10.1111/j.0014-3820.2006.tb00516.x

Rambaut, A., Suchard, M. A., Xie, D., & Drummond, A. J. (2014). *Tracer* v1.6. Retrieved from http://beast.bio.ed.ac.uk/Tracer (accessed 30 April 2019).

Rannala, B., & Yang, Z. (2003). Bayes estimation of species divergence times and ancestral population sizes using DNA sequences from multiple loci. *Genetics*, *164*, 1645–1656.

Reid, N. M., & Carstens, B. C. (2012). Phylogenetic estimation error can decrease the accuracy of species delimitation: A Bayesian implementation of the general mixed Yule-coalescent model. *BMC Evolutionary Biology*, *12*, 196. doi:10.1186/1471-2148-12-196

Rollinson, H. (2017). Masirah – the other Oman ophiolite: A better analogue for mid-ocean ridge process? *Geoscience Frontiers*, *8*, 1253–1262. doi:10.1016/j.gsf.2017.04.009

Ronquist, F., Teslenko, M., van der Mark, P., Ayres, D. L., Darling, A., Höhna, S., … Huelsenbeck, J. P. (2012). MrBayes 3.2: Efficient Bayesian phylogenetic inference and model choice across a large model space. *Systematic Biology*, *61*, 539–542. doi:10.1093/sysbio/sys029

Schluter, D. (1988). The evolution of finch communities on islands and continents: Kenya vs. Galapagos. *Ecological Monographs*, *58*, 229–249. doi:10.2307/1942538

Schluter, D. (2000). *The ecology of adaptive radiation*. Oxford: Oxford University Press.

Shackleton, R. M., & Ries, A. C. (1990). Tectonics of the Masirah fault zone and eastern Oman. *Geological Society, London, Special Publications*, *49*, 715–724. doi:10.1144/GSL.SP.1992.049.01.43

Silvestro, D., & Michalak, I. (2012). raxmlGUI: A graphical front-end for RAxML. *Organisms Diversity & Evolution*, *12*, 335–337. doi:10.1007/s13127-011-0056-0

Simó-Riudalbas, M., Metallinou, M., de Pous, P., Els, J., Jayasinghe, S., Péntek-Zakar, E., … Carranza, S. (2017). Cryptic diversity in *Ptyodactylus* (Reptilia: Gekkonidae) from the northern Hajar Mountains of Oman and the United Arab Emirates uncovered by an integrative taxonomic approach. *Public Library of Science One*, *12*, e0180397. doi:10.1371/journal.pone.0180397

Simó-Riudalbas, M., Tarroso, P., Papenfuss, T., Al-Sariri, T., & Carranza, S. (2018). Systematics, biogeography and evolution of *Asaccus gallagheri* (Squamata, Phyllodactylidae) with the description of a new endemic species from Oman. *Systematics and Biodiversity*, *16*, 323–339. doi:10.1080/14772000.2017.1403496

Sindaco, R., & Jeremčenko, V. K. (2008). *The reptiles of the Western Palearctic: Annotated checklist and distributional atlas of the turtles, crocodiles, amphisbaenians and lizards of Europe, North Africa, Middle East and Central Asia.* Latina: Edizioni Belvedere.

Sindaco, R. (2012). The IUCN red list of threatened species 2012: *Pristurus minimus*, e.T199590A2605302. Retrieved from http://www.iucnredlist.org/details/199590/0 (accessed 1 April 2019).

Smewing, J. D., Abbotts, I. L., Dunne, L. A., & Rex, D. C. (1991). Formation and emplacement ages of the Masirah ophiolite, Sultanate of Oman. *Geology*, *19*, 453–456. doi:10.1130/0091-7613(1991)019<0453:FAEAOT>2.3.CO;2

Šmíd, J., Carranza, S., Kratochvíl, L., Gvoždík, V., Nasher, A. K., & Moravec, J. (2013a). Out of Arabia: A complex biogeographic history of multiple vicariance and dispersal events in the gecko genus *Hemidactylus* (Reptilia: Gekkonidae). *Public Library of Science One*, *8*, e64018. doi:10.1371/journal.pone.0064018

Šmíd, J., Moravec, J., Kratochvíl, L., Gvoždík, V., Nasher, A. K., Busais, S. M., … Carranza, S. (2013b). Two newly recognized species of *Hemidactylus* (Squamata, Gekkonidae) from the Arabian Peninsula and Sinai, Egypt. *ZooKeys*, *355*, 79–107. doi:10.3897/zookeys.355.6190

Šmíd, J., Moravec, J., Kratochvíl, L., Nasher, A. K., Mazuch, T., Gvoždík, V., & Carranza, S. (2015). Multilocus phylogeny and taxonomic revision of the *Hemidactylus robustus* species group (Reptilia, Gekkonidae) with descriptions of three new species from Yemen and Ethiopia. *Systematics and Biodiversity*, *13*, 346–368. doi:10.1080/14772000.2014.996264

Šmíd, J., Shobrak, M., Wilms, T., Joger, U., & Carranza, S. (2017). Endemic diversification in the mountains: Genetic,

morphological, and geographical differentiation of the *Hemidactylus* geckos in southwestern Arabia. *Organisms Diversity & Evolution*, *17*, 267–285.

Stephens, M., & Scheet, P. (2005). Accounting for decay of linkage disequilibrium in haplotype inference and missing-data imputation. *The American Journal of Human Genetics*, *76*, 449–462. doi:10.1086/428594

Stephens, M., Smith, N. J., & Donnelly, P. (2001). A new statistical method for haplotype reconstruction from population data. *The American Journal of Human Genetics*, *68*, 978–989. doi:10.1086/319501

Tajima, F. (1989). Statistical method for testing the neutral mutation hypothesis by DNA polymorphism. *Genetics*, *123*, 585–595.

Tamar, K., Carranza, S., Sindaco, R., Moravec, J., Trape, J. F., & Meiri, S. (2016a). Out of Africa: Phylogeny and biogeography of the widespread genus *Acanthodactylus* (Reptilia: Lacertidae). *Molecular Phylogenetics and Evolution*, *103*, 6–18. doi:10.1016/j.ympev.2016.07.003

Tamar, K., Metallinou, M., Wilms, T., Schmitz, A., Crochet, P.-A., Geniez, P., & Carranza, S. (2018). Evolutionary history of spiny tailed lizards (Agamidae: *Uromastyx*) from the Saharo-Arabian region. *Zoologica Scripta*, *47*, 159–173. doi:10.1111/zsc.12266

Tamar, K., Mitsi, P., & Carranza, S. (2019). Cryptic diversity revealed in the leaf-toed gecko *Asaccus montanus* (Phyllodactylidae) from the Hajar Mountains of Arabia. *Journal of Zoological Systematics and Evolutionary Research*, *57*, 369–382. doi:10.1111/jzs.12258

Tamar, K., Scholz, S., Crochet, P.-A., Geniez, P., Meiri, S., Schmitz, A., … Carranza, S. (2016b). Evolution around the Red Sea: Systematics and biogeography of the agamid genus *Pseudotrapelus* (Squamata: Agamidae) from North Africa and Arabia. *Molecular Phylogenetics and Evolution*, *97*, 55–68. doi:10.1016/j.ympev.2015.12.021

Uetz, P., Freed, P., & Hošek, J. (2019). The reptile database. Retrieved from http://www.reptile–database.org (accessed 1 April 2019).

Vasconcelos, R., & Carranza, S. (2014). Systematics and biogeography of *Hemidactylus homoeolepis* Blanford, 1881 (Squamata: Gekkonidae), with the description of a new species from Arabia. *Zootaxa*, *3835*, 501–527. doi:10.11646/zootaxa.3835.4.4

Vu, V. Q. (2011). *ggbiplot: A ggplot2 based biplot. R package* version 0.55. Retrieved from http://github.com/vqv/ggbiplot/ (accessed 30 April 2019).

Williams, E. E. (1972). The origin of faunas. Evolution of lizard congeners in a complex island fauna: A trial analysis. *Evolutionary Biology*, *6*, 47–89.

Yang, Z. (2015). The BPP program for species tree estimation and species delimitation and species delimitation. *Current Zoology*, *61*, 854–865. doi:10.1093/czoolo/61.5.854

Yang, Z., & Rannala, B. (2010). Bayesian species delimitation using multilocus sequence data. *Proceedings of the National Academy of Sciences*, *107*, 9264–9269. doi:10.1073/pnas.0913022107

Yoder, J. B., Clancey, E., Des Roches, S., Eastman, J. M., Gentry, L., Godsoe, W., … Harmon, L. J. (2010). Ecological opportunity and the origin of adaptive radiations. *Journal of Evolutionary Biology*, *23*, 1581–1596. doi:10.1111/j.1420-9101.2010.02029.x

Associate Editor: Mark Wilkinson

Copyright of Systematics & Biodiversity is the property of Taylor & Francis Ltd and its content may not be copied or emailed to multiple sites or posted to a listserv without the copyright holder's express written permission. However, users may print, download, or email articles for individual use.